IEEE Access
Multidisciplinary | Rapid Review | Open Access Journal

Received April 27, 2018, accepted June 7, 2018, date of publication June 22, 2018, date of current version July 12, 2018.

Digital Object Identifier 10.1109/ACCESS.2018.2849697

Multi-Frequency Test Generation for Incipient Faults in Analog Circuits Based on the Aliasing Measuring Model

YANG YU, (Member, IEEE), YUEMING JIANG, AND XIYUAN PENG
Department of Instrument Science and Technology, Harbin Institute of Technology, Harbin 150001, China
Corresponding author: Yueming Jiang (yueming07050106@163.com)

This work was supported by the National Natural Science Foundation of China under Grant 61571161.

ABSTRACT A novel method of generating multi-frequency test stimuli for incipient faults is presented to improve the fault detection accuracy of analog circuits. This paper analyzes the primary cause of low incipient fault detection accuracy and indicates that the high aliasing between the incipient fault response and the normal response seriously impairs the fault recognition ability of fault classifiers. Therefore, this paper builds an aliasing measuring model (AMM) to generate the multi-frequency test stimuli set for incipient faults. The principle part of the AMM is the aliasing measuring algorithm (AMA), which uses the response aliasing as the pivotal index to evaluate the test frequency. The test frequencies with smaller response aliasing will be selected. The other part of the AMM contains the genetic algorithm and the greedy algorithm, which can advance the AMA to quickly generate the multi-frequency test stimuli set for the incipient fault and can ensure that the obtained test set covers the entire circuit and contains fewer test frequencies. The simulation experimental results validate two conclusions: the test frequencies obtained by the AMM remarkably increase the incipient fault detection accuracy and reduce the time for test frequency generation and the multi-frequency test stimuli set contains fewer elements. The hardware experimental results demonstrate that the proposed method is practicable and effective.

INDEX TERMS Analog circuits, incipient fault, multi-frequency test generation, aliasing measuring model.

I. INTRODUCTION

The electronic systems have been applied to many important fields including Aerospace Engineering, Arms Industry, Nuclear Power, etc. In electronic systems, most faults are caused by analog circuits. Although the area of the analog circuits is smaller than the digital section, and the fault detection and diagnosis of analogs circuits is more difficult than that of digital circuits because of the continuous state, nonlinear correspondence and component tolerance of analog circuits. Therefore, fault detection and diagnosis for analog circuits remains a considerable challenge.

At present, the methods of analog fault detection and diagnosis mainly focus on the hard fault and soft fault [1]–[3], caused by large parametric deviations of the component. These faults result in observable changes of the circuit state and reach the fault performance threshold; thus, they have attracted considerable research attention. However, certain faults may have occurred before reaching the fault threshold. This type of fault is called the incipient fault in this paper, and they occur in two stages of the analog circuit lifecycle. The first stage is the manufacturing integrated circuit (IC). For IC production lines, the structural test and functional test, as two main test methods, have been conducted to ensure the analog circuit operate normally. However, the incipient fault detection is not employed in the production lines, and the incipient faults may not be detected by the structural test and functional test. The causes of these faults are subtle parametric deviations derived from component defects and the increasing equivalent resistance derived from the cold solder joint. When operating in the working state, ICs existing incipient fault have a higher likelihood of occurring hard or soft fault and lower reliability compared with normal circuits. The second stage is applying the circuit to the actual field. The parameters of the components will degrade under many types of stresses after the increasing working hours, including voltage, temperature, humidity and radiation stresses. For example, Kulkarni *et al.* [4]–[6] monitored the performance of electrolytic capacitors in DC/DC convertors for 650 hours. The results showed that the capacitance decreased and the Equivalent Series

2169-3536 © 2018 IEEE. Translations and content mining are permitted for academic research only.
Personal use is also permitted, but republication/redistribution requires IEEE permission.
See http://www.ieee.org/publications_standards/publications/rights/index.html for more information.

Resistance (ESR) increased gradually, which led to increasing the ripple amplitude of the output DC signal.

Although the effects of the incipient fault on the performance of the analog circuit are barely observed, if the incipient fault is not identified and prevented, then the growing parametric deviation of the components will increase the likelihood that the incipient fault develops a sudden circuit failure. Especially for IC production lines, the effective identification of the incipient fault can alter the operator and reduce the impairment of the circuit performance. Meanwhile, the incipient fault detection has no effect on the yield loss, the fault detection results are considered as the warnings, which express that ICs with the incipient faults will have a higher likelihood of occurring hard or soft fault. Hence, the yield loss will not increase.

The incipient fault usually does not have a significant influence on the circuit performance, but it still represents a type of analog fault. Based on the methods improving fault identification, including the test stimulus and test node selection strategy, the optimized feature extraction method and the fault classifier strategy, this paper focuses on test stimulus selection for incipient faults. Generating multi-frequency test stimuli can increase the difference between the normal response and the incipient fault response and excite the subtle incipient fault features to improve the fault detection accuracy.

In the field of fault detection and diagnosis in analog circuits, test stimuli can be divided into DC and AC signals. The DC signal is appropriate for hard faults in linear analog circuits but does not present the excitation on soft faults. Milor and Visvanathan [7] and Devarayanadurg and Soma [8] selected a series of DC signals as test stimuli and applied them to the test circuit. The pulse signal [9], [10] is commonly used for AC test stimuli because it can be decomposed into harmonic waves with different frequencies. However, when a pulse stimulus excites the incipient fault, the fault detection accuracy is low and a higher sampling frequency is needed to obtain the response signals, which can increase the hardware costs. Based on this situation, many methods have been proposed to select the test stimulus for the faults in the analog circuit, such as the sinusoidal waves corresponding to the selected test frequencies will be used to excite the faults more efficiently and improve the fault detection accuracy. Marin [11] adopted a sensitivity analysis combined with entropy criteria to obtain the optimum set of frequencies. Sun *et al.* [12] presented an approach for feature selection using the criteria for maximum relevance Minimum Redundancy (MR) and Support Vector Machines (SVMs). Bentobache *et al.* [13] showed that minimizing the number of test frequencies for linear analog circuits can be modeled as a set-covering problem. Kincl and Kolka [14] proposed a new control mechanism based on a penalty function that can give more regularly distributed test frequencies over the entire frequency band. Yang *et al.* [15] built a complex field fault model that can adjust the frequency of the input signal so that the model can be in an optimum state to select the optimal test frequencies. Puvaneswari *et al.* [16] used multiple frequency measurements to detect multiple soft faults in linear analog circuits. In [17], the paper presented a methodology for algorithmic generation of test signals for the detection and diagnosis of a variety of short and open-circuit defects in analog circuits.

In summary, the above methods mainly focus on hard and soft faults caused by large parametric deviations of the components. When these methods are used to select the test frequencies for incipient faults, the selected test stimuli set does not present significant excitation on the incipient faults, which results in low fault detection accuracy. In addition, the scale of the test stimuli set is too large to be applied to the actual circuit. The primary reason why these methods are unsuitable for incipient fault is that the evaluation indexes used in these methods cannot express the essence of low incipient fault detection accuracy. Specifically, the essence is high aliasing between the normal response and incipient fault response. Even by extracting the fault feature, the fault classifier still cannot separate the incipient fault feature from the normal feature very well.

Based on this problem, this paper selects aliasing as the evaluation index and proposes the Aliasing Measuring Model (AMM) to generate the test frequencies. The model analyzes the statistical characteristics of the frequency characteristic curves of normal samples and incipient fault samples. The analysis results show that the normal samples and incipient fault samples in a single test frequency approximately obey a normal distribution, respectively; therefore, they can be described as two different normal distribution curves. Overlapping area between two curves indicates the aliasing will vary when the test frequency changes. Thus, the Aliasing Measuring Algorithm (AMA), which is the principle part of the AMM, is presented to select the test frequency. Then, the AMA is combined with the Genetic Algorithm (GA) to obtain the test frequencies for all incipient faults by minimizing the aliasing. Finally, the multi-frequency test stimuli set is generated with the Greedy Algorithm (GRA) for the entire circuit. The advantages of the proposed method are as follows:

1) Exciting all types of faults, especially for incipient faults presenting excellent excitation;

2) Improving the speed of selecting the test frequencies;

3) Simplifying the multi-frequency test stimuli set without redundancy;

4) Requiring a lower sampling frequency and hardware cost than the pulse stimulus;

5) Not needing a complex feature extraction method (e.g., wavelet analysis) and only needing a transformation from the time domain to the frequency domain using the Fast Fourier Transform (FFT).

II. METHOD OF MULTI-FREQUENCY TEST GENERATION

This paper proposes a method of multi-frequency test generation based on the AMM. The AMA is the principle part of the model and calculates the values of the Aliasing

Function (AF) over all test frequencies. The AMA is combined with the other parts of the AMM, including the GA and GRA, to quickly generate the multi-frequency test stimuli corresponding to the minimum total of the AF and covering the entire circuit.

A. ALIASING MEASURING ALGORITHM

1) MOTIVATION

In analog circuit, the incipient faults may be mainly caused by the solder joint oxide, cold solder joint, the fracture of PCB and the parameter deviation of the components. According to [18]–[20], the effect deriving from the solder joint oxide, cold solder joint and the fracture of PCB on the analog circuit can be equivalent to the parameter deviation of the components, such as increasing the equivalent resistance. Hence, the parameter deviation of the components can be considered as the main source of the incipient fault in this paper. For each component, there is the maximum allowed normal parameter deviation, the incipient faults may exist when the parameter deviation is more than the maximum allowed normal deviation. In this paper, the maximum allowed normal deviation is set to the tolerance of each component, which causes the incipient fault and is used to select the test frequencies. This ensures that the obtained test frequencies can excite all faults caused by the parameter deviation that is more than the maximum allowed normal parameter deviation.

Firstly, to establish the relationship between the output feature and test frequency, for the normal state and the incipient fault state caused by the maximum allowed normal parameter deviation, this paper obtains the frequency characteristic curves consisting of the amplitude-frequency curves and phase-frequency curves. Which describe the amplitude and phase, respectively, of the output samples over each test frequency. Then, it is well known that the parameter in the tolerance of the component obeys the normal distribution, and the output response of analog circuit, which is composed of a certain number of components, approximately obeys the normal distribution according to the law of large numbers. Hence, for one incipient fault, when the number of frequency characteristic curves is sufficiently large. By analyzing the statistical characteristics of the normal samples and incipient fault samples in a single test frequency, the samples can be fitted into two different normal distribution curves. The normal distributions at different frequencies are obtained through simulations using an AC sweep and Monte Carlo analysis, the simulation results can be directly applied into the actual circuit, because the frequency characteristic curves of the analog circuit basically remain unchanged between the simulations and the experimental measurements. For example, the circuit of the Sallen-key filter is shown in Fig. 1. The amplitude-frequency curves are obtained using an AC sweep and 300 Monte Carlo analysis that obeys the Gaussian distribution, the incipient fault is caused by a -10 % parametric deviation C1, and the amplitude-frequency curves are shown in Fig.2.

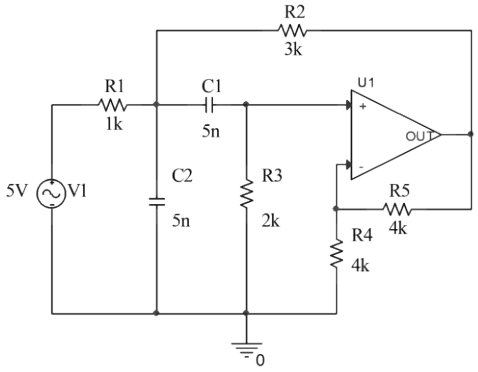

FIGURE 1. Schematic of Sallen-key Filter Circuit.

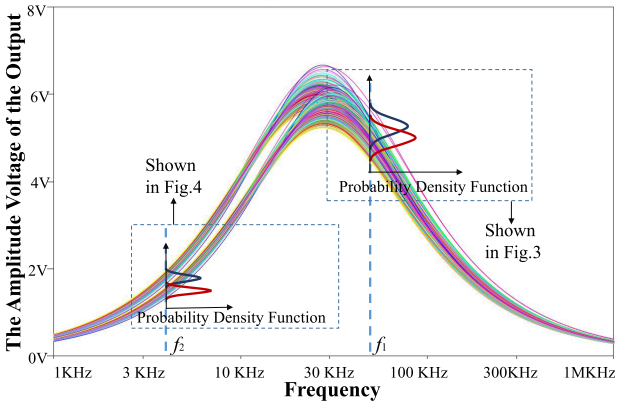

FIGURE 2. Amplitude-frequency curves of the normal and incipient fault samples.

In Fig.2, the horizontal axis indicates the frequency and the vertical axis indicates the voltage amplitude of the output. The voltage amplitude of the normal and incipient samples will obey the normal distribution in each test frequency, such as the f_1 test frequency and the f_2 test frequency. Fig.3 and Fig.4 show the fitting normal distribution curves of normal samples and incipient samples in the f_1 and the f_2 test frequency.

In Fig. 3 and Fig. 4, the horizontal axis indicates the voltage amplitude and the vertical axis indicates the probability density function. Obviously, the overlapping area in the f_1 test frequency is larger than that in the f_2 test frequency. Thus, distinguishing the fault and normal samples will be more difficult in the f_1 test frequency than in the f_2 test frequency. The overlapping area between these two curves will change in different test frequencies; therefore, this paper presents the test frequency selection principle based on the AMA. The selected test stimuli correspond to the minimum of the overlapping area, i.e., the smallest value of the AF.

2) ALGORITHM PRINCIPLE

The principle of the AMA is as follows. First, the frequency characteristic curves (amplitude-frequency curves and phase-frequency curves) will be obtained for the normal state and the incipient fault state. Then the amplitude and phase of the

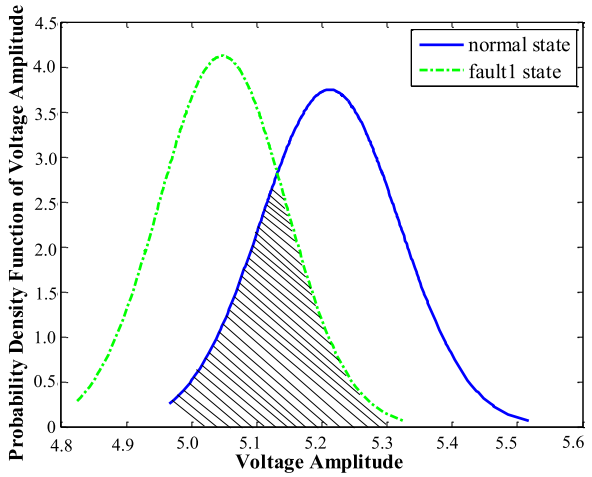

FIGURE 3. Normal distribution curves of the normal and fault samples in the f_1 test frequency.

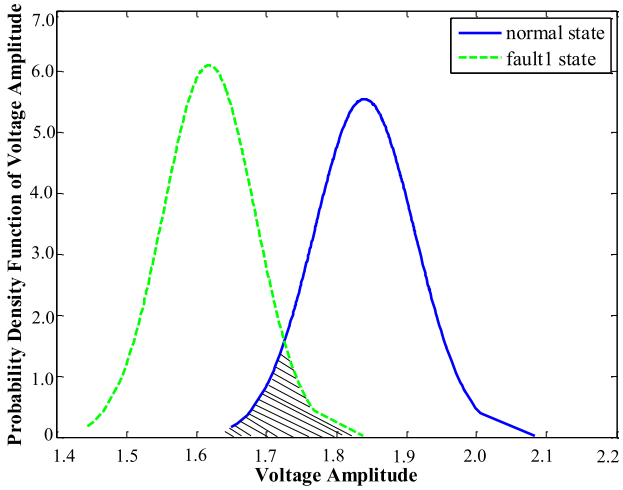

FIGURE 4. Normal distribution curves of the normal and fault sample in the f_2 test frequency.

normal samples and incipient fault samples obey the normal distribution in each test frequency, and the overlap area is different. Fig.5 describes this process.

In Fig.5, it assumed that the normal samples obey the normal distribution $N(\mu_1, \sigma_1^2)$, and the incipient fault samples obey the normal distribution$N(\mu_2, \sigma_2^2)$. For the entire frequency band, the number of the test frequencies is N, the test frequencies are denoted as $f_1 \ldots f_N$. Finally, the optimal test frequency will be selected by comparing the overlapping area, the calculating process of the overlapping area is as follows.

When the fault happens in analog circuit, which will result in the performance deviation of the fault state may be higher or lower than the normal state, so there are two types of positions between the normal sample curve and the fault sample curve in Fig.5. x_1 and x_2 express the abscissa of the intersection points between the normal samples and the incipient fault samples, and they are then combined with the

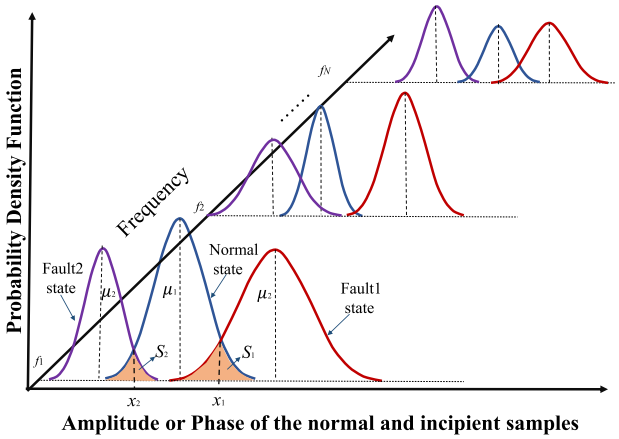

FIGURE 5. Normal distribution curves for the normal samples and two types of fault samples.

integral of normal distribution curves of the normal and fault samples to calculate the overlapping area. The expressions of the normal distribution function of the normal and the fault samples are shown in Eq. (1) and Eq. (2). The area enclosed by the normal distribution curve and the horizontal axis can be calculated using Eq. (3) and Eq. (4), namely the integral of normal distribution curves. Where, x manifests the amplitude or phase of output.

$$y_1(x) = \frac{1}{\sigma_1\sqrt{2\pi}} e^{-\frac{(x-\mu_1)}{2\sigma_1^2}} \tag{1}$$

$$y_2(x) = \frac{1}{\sigma_2\sqrt{2\pi}} e^{-\frac{(x-\mu_2)}{2\sigma_2^2}} \tag{2}$$

$$S_{Normal} = \int_{-\infty}^{+\infty} y_1(x)dx = 1 \tag{3}$$

$$S_{Fault} = \int_{-\infty}^{+\infty} y_2(x)dx = 1 \tag{4}$$

The position of the normal distribution curves between the normal state and the Fault1 state in Fig. 5 indicates that the performance deviation of the fault state is higher than the normal state. That means $\mu_1 < \mu_2$, the overlapping area S_1 is expressed as Eq. (5).

$$S_1 = \int_{x_1}^{+\infty} y_1(x)dx + \int_{-\infty}^{x_1} y_2(x)dx, \quad \mu_1 < \mu_2 \tag{5}$$

The position of the distribution curves between the normal state and the Fault2 state in Fig. 5 indicates that the performance deviation of the fault state is lower than the normal state. When $\mu_1 > \mu_2$, The overlapping area S_2 is expressed as Eq. (6).

$$S_2 = \int_{-\infty}^{x_2} y_1(x)dx + \int_{x_2}^{+\infty} y_2(x)dx, \mu_1 > \mu_2 \tag{6}$$

Then, for each test frequency, $f_i(i = 1 \ldots N)$, the overlapping area manifests the aliasing between the normal samples and the incipient fault samples, namely the value of AF, denotes $AF(f_i)$, so AF is defined as Eq. (7).

$$AF(f_i) = \begin{cases} S_1(f_i) = \int_{x_1}^{+\infty} y_1(x(f_i))dx + \int_{-\infty}^{x_1} y_2(x(f_i))dx, \mu_1 < \mu_2 \\ S_2(f_i) = \int_{-\infty}^{x_2} y_1(x(f_i))dx + \int_{x_2}^{+\infty} y_2(x(f_i))dx, \mu_1 > \mu_2 \end{cases} \tag{7}$$

Where, x (f_i) means the value of the amplitude or phase of the output, the value of AF is calculated using the integral of normal distribution curves, so the value of AF is in a range of (0,1). The selected test frequency f_{best} minimizes the $AF(f_i)$, which is denoted as $AF(f_{best})$, i.e., $AF(f_{best}) = \min(AF(f_i))$.

Every component in the analog circuit has specific effects on the circuit performance. When the faults are caused by different components, the sensitive feature (i.e., amplitude or phase) is diverse. Based on this rule, the feature with a smaller $AF(f_{best})$ value is chosen as the sensitive feature. D1 is assumed to be the value of $AF(f_{best})$ obtained from the amplitude of the samples, and D2 is assumed to be the value of $AF(f_{best})$ obtained from the phase. When D1<D2, the amplitude is considered as the sensitive feature and the frequency corresponding to D1 is selected. Otherwise, the phase is considered as the sensitive feature and the frequency corresponding to D2 is selected.

B. GENETIC ALGORITHM

When selecting the test frequency, the exhaustive search increases the runtime and number of calculations because of the large number of test frequencies. Therefore, the GA search, which presents an excellent search ability, is used to quickly select the test frequency. The GA search is described as follows.

1) The encoded mode of the test frequencies is set as binary. The number of all test frequencies is N; therefore, the encoded digit n identifies the least positive integer that makes $2^n > N$ be reasonable. Every n digits of binary code represent the gene of the individual.

2) Set the fitness function. In each generation, the fitness of every individual in the population is evaluated, which is the value of the fitness function in the optimization problem. Individuals with greater fitness are stochastically selected from the current population. The AF is the objective function, which needs to perform certain mathematical operations to form the fitness function in this paper. The detailed operation is described in Eq. (8).

$$\text{Fitness}(f_i) = 1/AF(f_i) \tag{8}$$

3) Design the genetic operators. The type of selected operator is proportionate selection, namely roulette-wheel selection. The modes of the crossover operator and mutation operator are the single-point crossover and simple mutation, respectively.

4) The test frequency selection process is based on the AMA combined with the GA as follows.

Step 1: Perform binary encoding and parameter initialization. The parameters include the population, generation, crossover probability and mutation probability.

Step 2: Calculate the fitness values of the individuals. The genes will be selected, crossed and mutated to produce the new generation.

Step 3: Terminate the algorithm when the maximum number of generations has been produced. The results are the optimal test frequency and the corresponding $AF(f_{best})$ value.

Step 4: Compare the $AF(f_{best})$ values between the amplitude and phase, and select the smaller value as the sensitive feature and the corresponding f_{best} as the optimal test frequency.

C. GREEDY ALGORITHM

The test frequencies are selected using the AMA combined with the GA. However, for actual circuits, the number of the selected test frequencies is too large; therefore, the GRA can be used to reduce the scale of test frequencies. The incipient fault feature will be the most prominent in its optimal test frequency, however, the other test frequencies may also have prominent excitations. For example, the optimal test frequencies of Fault1 and Fault2 in the Leapfrog circuit are $f_1 = 1,147$ Hz and $f_2 = 1,186$ Hz. The frequency values are fairly close; therefore, both Fault1 and Fault2 can be excited by either f_1 or f_2.

The selection of the multi-frequency test stimuli set will be changed into a weighted set-covering problem. The first step is building the initial matrix $\mathbf{A}$. The row vectors are the selected test frequencies, which are denoted as $f_i(i = 1, 2..m)$, and the column vectors are all the incipient faults caused by the parametric deviation of the components in the analog circuit, which are denoted as $IF_j(j = 1, 2..n)$. Each element A_{ij} indicates the AF value in the corresponding test frequency for the incipient fault. For example, A_{12} is the AF value in the f_1 test frequency forIF_2. The weight value of the row vector is the summation of the AF values for all incipient faults in every test frequency, which are denoted as SAF. An example is given to describe the initial matrix in Table 1. The number of incipient faults is five, which are denoted as $IF_j(j = 1, 2..5)$, and the corresponding five test frequencies are denoted as $f_i(i = 1, 2..5)$.

TABLE 1. Initial matrix.

	IF_1	IF_2	IF_3	IF_4	IF_5	SAF
f_1	0.0466	0.9067	0.8412	0.0451	0.4558	2.2954
f_2	0.6420	0.1387	0.1386	0.6513	0.1116	1.6822
f_3	0.6272	0.1392	0.1387	0.6366	0.1512	1.6929
f_4	0.0468	0.8067	0.8061	0.0449	0.4628	2.1673
f_5	0.6165	0.6458	0.5479	0.6255	0.0743	2.5100

The second step is changing the initial matrix into a 0-1 matrix **B**, where element '1' indicates the test frequency that can excite the incipient fault and '0' indicates the opposite. Two rules are established to change A_{ij} into element '1' or '0'. First, when the$AF(f_{best})$ for one fault is much less than 0.1, the test frequencies whose AF values are more than 0.1 are considered to have no excitation on this fault, and the corresponding A_{ij} are changed to '0'. Second, when the $AF(f_{best})$ for one fault is more than 0.1, the test frequencies whose AF values are more than twice the $AF(f_{best})$ are not taken into consideration. The corresponding A_{ij} are changed to element '0'. The 0-1 matrix **B** based on the above two rules is given in Table 2.

TABLE 2. 0-1 matrix.

	IF_1	IF_2	IF_3	IF_4	IF_5	SAF	v
f_1	1	0	0	1	0	2.2954	1.1477
f_2	0	1	1	0	0	1.6822	0.8411
f_3	0	1	1	0	0	1.6929	0.8465
f_4	1	0	0	1	0	2.1673	1.0837
f_5	0	0	0	0	1	2.5100	2.5100

The objective of the GRA is that the selected row vectors can successively cover all the column vectors and maintain the minimum summation of the SAF for the selected row vectors. The Boolean variable P records the coverage of the column vectors. When the jth column is covered, $P_j =$ true, or $P_j =$ false ($j = 1, 2, \ldots n$). In addition, c_i is the weight value (SAF) of ith row vector, and v_i is the average weight value, which is the evaluated index in the GRA, and it is calculated using Eq. (9).

$$v_i = \frac{c_i}{\sum_{j=1,Pj=false}^{n} \mathrm{B}_{ij}} \tag{9}$$

The selection principle is shown as follows. For the 0-1 matrix, the row vector (test frequencies) with the minimum v is selected to cover the column vectors (incipient faults). Then, the selected row vector and covered column vectors are eliminated from the matrix, which will be changed into a new 0-1 matrix. The selection will continue from this new matrix until all column vectors have been covered. All successive selected test frequencies are the multi-frequency test stimuli set for the entire circuit. To examine whether the test frequency set contains redundancy, any one test frequency f_x is first removed from the set, which leads to p classes of incipient faults that are not covered. If one or more elements in the remaining set can cover the same p classes of incipient faults, then f_x must be eliminated from the test stimuli set; otherwise, the test frequency set does not present redundancy.

Based on the above selection principle and examination method, the first selected frequency for the matrix in Table 2 is f_2. Then, the second row and the second and third columns are eliminated. The second selected frequency is f_4, and the third one is f_5. All columns have been covered by these three frequencies; therefore, the test frequency set is $\{f_2, f_4, f_5\}$. The resulting summation of the SAF is 6.3595. According to the examination method, this test frequency set does not present redundancy.

D. PROCEDURE OF MULTI-FREQUENCY TEST GENERATION

The detailed procedure of the multi-frequency test generation based on the proposed AMM is described in Fig. 6.

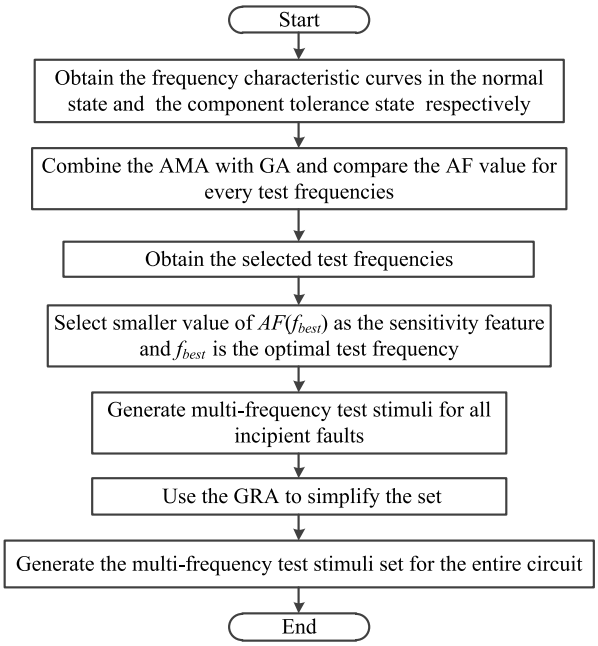

FIGURE 6. Procedure of multi-frequency test generation.

First, the frequency characteristic curves in the normal state and the component tolerance sate are obtained from the analog circuit. Then, the AMM generates the multi-frequency test stimuli set for the entire circuit. The AMA, as the pivotal component of the AMM, is combined with the GA to select the test stimuli set for every incipient fault. The GRA further simplifies the test stimuli set. Finally, multi-frequency test generation will be realized for all incipient faults in the entire circuit.

III. SIMULATION EXPERIMENT

A. LEAPFROG FILTER

A Leapfrog filter is a benchmark circuit of ITC97 that consists of 13 resistors, 4 capacitors and 6 operational amplifiers. The nominal values for all components are labeled in Fig. 7. The tolerance of the resistors and capacitors are set to 10% and 5%, respectively.

In section II, the maximum allowed normal deviation is set to the tolerance of the component, and the faults caused by the tolerance are shown in Table 3, denoted as F1-F17. The selected test frequencies excite all the incipient faults caused by more than the maximum allowed normal deviation. In this paper, all faults are caused by the fault parametric deviations

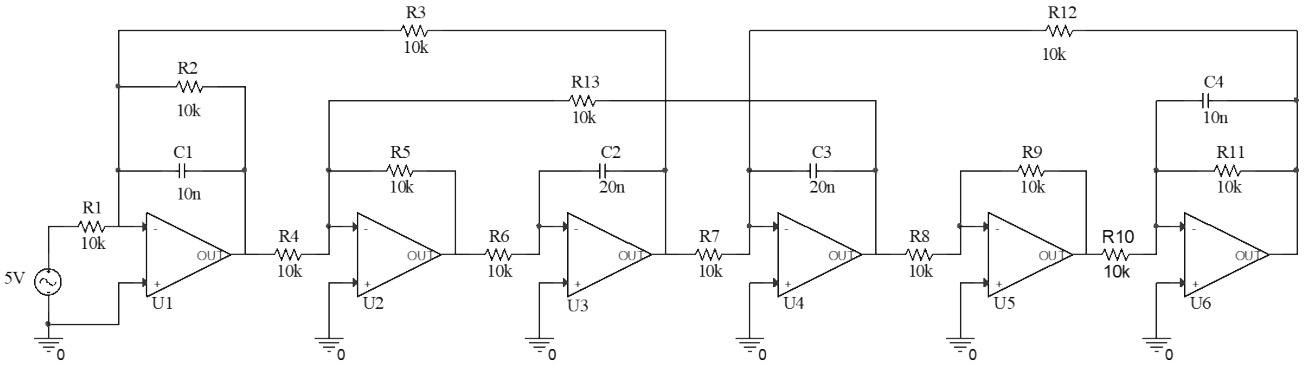

FIGURE 7. Schematic of leapfrog filter circuit.

TABLE 3. Sensitivity feature and optimal test frequency for all faults in the leapfrog circuit.

Fault	Fault component	Sensitive feature	Optimal test frequency(Hz)	$AF(f_{best})$
F1	C1	Phase	f_1=3069	0.00001
F2	C2	Phase	f_2=1147	0.03395
F3	C3	Phase	f_3=1186	0.03461
F4	C4	Phase	f_4=4054	0.00001
F5	R1	Amplitude	f_5=851	0.07440
F6	R2	Phase	f_6=5000	0.00347
F7	R3	Amplitude	f_7=885	0.05525
F8	R4	Amplitude	f_8=635	0.11418
F9	R5	Phase	f_9=1207	0.03372
F10	R6	Phase	f_{10}=753	0.02749
F11	R7	Amplitude	f_{11}=1182	0.08217
F12	R8	Amplitude	f_{12}=611	0.11544
F13	R9	Amplitude	f_{13}=5000	0.11944
F14	R10	Amplitude	f_{14}=603	0.08975
F15	R11	Phase	f_{15}=5000	0.01908
F16	R12	Amplitude	f_{16}=878	0.05956
F17	R13	Amplitude	f_{17}=467	0.03093

that is more than the maximum allowed normal deviation. To demonstrate the multi-frequency test stimuli exciting all faults caused by the different fault parametric deviations, it is assumed that the faults are divided into three types according to the degree of the fault parametric deviations. They are as follows: incipient fault [tolerance-±20%]; common fault [±20%-±50%]; and serious fault [±50%-±100%].

The amplitude and phase-frequency curves of the normal and incipient fault samples are obtained using an AC sweep analysis and Monte Carlo analysis with the Pspice 16.7 software. The amplitude of the AC sweep source is 5 V, and the sweep range is set to [300 Hz, 5 KHz], according to the Leapfrog filter pass band. Three hundred Monte Carlo analysis runs are performed for two types of samples using a Gaussian distribution. The AMA is combined with the GA to obtain the $AF(f_{best})$ of the amplitude and phase. The smaller $AF(f_{best})$ is selected as the sensitive feature, and the corresponding test frequency is the optimal test frequency. The results from the Leapfrog circuit are shown in Table 3.

In Table 3, every optimal test frequency can excite all faults caused by the fault parametric deviations of the corresponding component. Therefore, these 17 test frequencies can cover all the faults in the entire circuit. However, the large number of available test frequencies cannot be applied to an actual circuit. The GRA selects the multi-frequency test stimuli set from the 17 optimal test frequencies to cover the entire circuit. The first step in the GRA is to build the initial matrix. Then, the developed matrix will be converted into a 0-1 matrix based on the rules shown in Section III. The '1' elements are replaced by the corresponding incipient faults shown in Table 4.

TABLE 4. Matrix of the test frequencies covering incipient faults.

Test Frequency(Hz)	Covering the incipient faults	SAF
f_1=3069	{F1 F4 F6 F15}	0.03647
f_2=1147	{F1 F2 F3 F4 F9 F10}	0.28310
f_3=1186	{F1 F2 F3 F4 F9 F10}	0.26462
f_4=4054	{F1 F4 F6 F15}	0.02514
f_5=851	{F5 F8 F11 F12}	0.19156
f_6=5000	{F1 F4 F6 F15}	0.02256
f_7=885	{F5 F7 F8 F12 F13 F16 F17}	0.45460
f_8=635	{F5 F7 F8 F12 F13 F16 F17}	0.45376
f_9=1207	{F1 F4 F9 F10}	0.05570
f_{10}=753	{F1 F2 F3 F4 F9 F10}	0.30085
f_{11}=1182	{F2 F3 F4 F11 F12}	0.27908
f_{12}=611	{F5 F7 F8 F12 F13 F14 F16 F17}	0.44262
f_{13}=5000	{F1 F4 F8 F11 F13}	0.14313
f_{14}=603	{F5 F7 F8 F12 F13 F14 F16 F17}	0.43995
f_{15}=5000	{F1 F4 F6 F15}	0.02256
f_{16}=878	{F5 F7 F8 F12 F13 F14 F16 F17}	0.45215
f_{17}=467	{F4 F7 F8 F12 F13 F14 F16 F17}	0.44407

According to Eq. (9) and the selection principle of the GRA, the successively selected test frequencies are f_6, f_9, f_5, f_{14}, and f_3, which form the test stimuli set {5000 Hz, 1207 Hz, 851 Hz, 603 Hz, and 1186 Hz}, respectively, for the Leapfrog circuit. The summation of the SAF is 0.97438.

To illustrate the advantages of the multi-frequency test stimuli set, the following experiments are performed.

1) COMPARISON OF THE EXCITATION EFFECT ON THE INCIPIENT FAULT

The selected test frequencies can excite the incipient fault samples separated from the normal samples, and the separation state can evaluate the test stimulus.

The incipient fault is caused by a +20% parametric deviation of R1 in the Leapfrog circuit. Two types of test stimuli are compared: the multi-frequency test stimuli set and the pulse stimulus. 300 normal samples and incipient fault samples are extracted using the FFT. The amplitudes of the samples are set to the comparison values, and Fig. 8 describes the comparison results. The most appropriate extraction method for the pulse stimulus is the wavelet analysis. Therefore, 300 normal samples and incipient fault samples for the same two types of stimuli are extracted using the wavelet analysis. The comparison value is set to the fifth layer of the wavelet coefficients, and the results are shown in Fig. 9.

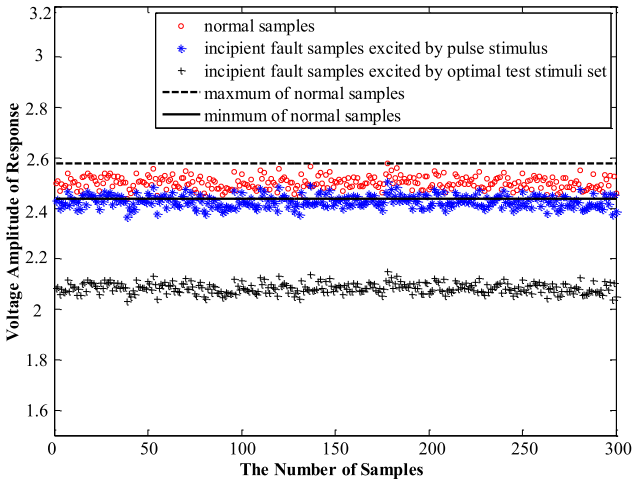

FIGURE 8. Comparison of the amplitudes of the normal and incipient fault samples.

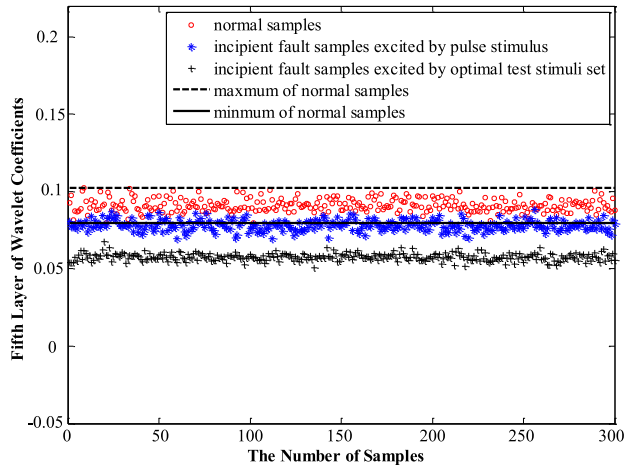

FIGURE 9. Comparison of the fifth layer of the wavelet coefficients for the normal and incipient fault samples.

Both Fig. 8 and Fig. 9 express that the separation state using the multi-frequency test stimuli set is better than that from the pulse stimulus. The paper proposes two indexes to quantify the separation state. One index is the distance between the normal and the incipient fault samples, and it is calculated as the absolute value of the difference between the average values of the normal and incipient fault samples and denoted as the D-value. The corresponding formula is shown in Eq. (10).

$$\text{D-value} = \left| (\sum_{i=1}^{n} NA_i - \sum_{i=1}^{n} FA_i)/n \right| \tag{10}$$

Where n represents the number of samples, NA_i represents the amplitude or fifth layer of the wavelet coefficients of the normal samples, and FA_i represents the amplitude of the incipient fault samples.

In Fig. 8 and Fig. 9, the distribution of the normal samples forms one data band between the maximum and minimum values; therefore, a second index shows the number of points of the incipient fault samples that fall into the normal data band, which is denoted as the P-value. This value can evaluate the aliasing between different samples. The values of the D-value and P-value corresponding to Fig. 8 and Fig. 9 are given in Table 5.

TABLE 5. The values of two indexes.

Corresponds to figure	Index	Multi-frequency test stimuli set & FFT	Pulse stimulus & FFT
Figure 8	D-vaule	0.4169	0.0729
	P-value	0	107
Corresponds to figure	Index	Multi-frequency test stimuli set & Wavelet Analysis	Pulse stimulus & Wavelet Analysis
Figure 9	D-vaule	0.0334	0.0127
	P-value	0	103

The experimental results shown in Figs. 8 and Fig. 9 and Table 5 demonstrate that the multi-frequency test stimuli set dramatically increased the distance and decreased the aliasing between the normal samples and incipient fault samples, regardless of the feature extraction method.

2) COMPARISON OF FAULT DETECTION ACCURACY

The incipient faults are caused by the parametric deviation of the components, and one or more components may simultaneously exist the parametric deviation, the selected test stimuli set can excite the incipient fault as well as common and serious faults. The fault sets are shown in Table 6.

For the faults sets in Table 6, a comparison of the fault detection accuracy is conducted between the multi-frequency test stimuli set and the pulse stimulus. The Support Vector Data Description (SVDD) is chosen as the fault classifier. First, the sine waves corresponding to the multi-frequency test stimuli set excite the faults in Table 6. Then, 600 normal samples and 300 fault samples of every type of fault are extracted using FFT. The 300 extracted normal samples are used as the training data of the SVDD, and another 300 extracted normal samples and faults are used as the testing data. Fault detection is performed using a pulse stimulus combined with a wavelet analysis as the

TABLE 6. Fault sets in leapfrog circuit.

Fault	Number of fault components	Fault type	Fault components	Parameter deviation ratio
Faut1	Single	Incipient	C1	-10%
Faut2	Single	Incipient	C4	-9%
Faut3	Single	Incipient	R1	+10%
Faut4	Single	Incipient	R2	+12%
Faut5	Single	Incipient	R11	+15%
Fault6	Multiple	Incipient	C2 R6	-8% +10%
Fault7	Multiple	Incipient	C3 R5	-10% +12%
Fault8	Multiple	Incipient	R3 R8	+11% +15%
Fault9	Multiple	Incipient	R4 R12	+14% +13%
Fault10	Multiple	Incipient	R7 R9	+20% +10%
Fault11	Multiple	Incipient	R10 R13	+15% +10%
Faut12	Single	Serious	C1	-60%
Faut13	Single	Serious	C3	-85%
Faut14	Single	Common	R3	+23%
Faut15	Single	Common	R6	+35%
Faut16	Single	Common	R13	+48%

comparison experiment. The comparison results are given in Table 7 and Table 8.

The results from Table 7 and Table 8 can be summarized as follows. (1) The multi-frequency test stimuli set can excite the incipient fault regardless of the number of the fault components. (2) The excitation of the incipient fault of the multi-frequency test stimuli set is stronger than that of the pulse stimulus. The average fault detection accuracy reaches 97.64%, which is 45.65% higher than that of the pulse stimulus. (3) The multi-frequency test stimuli set has the same strong excitation on common and serious faults, where the average fault detection accuracy reaches 99.13%. (4) The average normal detection accuracy cannot reach 100% because of the fall-out ratio of the SVDD. The above conclusions strongly demonstrate that the multi-frequency test stimuli set can excite all faults and dramatically increase the incipient detection accuracy.

3) COMPARISON OF THE RUNNING TIMES OF THE GENERATED TEST FREQUENCY

The method of selecting the test frequency based on the AMM is a GA search instead of an exhaustive search to decrease the running time. The comparison experiment is conducted between the GA search and exhaustive search for Fault1 in Table 6. The results, including the running time and fault detection accuracy, are shown in Fig. 10 and Fig. 11, respectively. The running time for the GA search is far less than that of the exhaustive search, with the former approximately one tenth the value of the latter; however, the incipient fault detection accuracy is unaffected.

TABLE 7. Incipient fault detection accuracy with two types of test Stimuli.

Fault Sets	Multi-frequency test stimuli set & FFT		Pulse stimulus & Wavelet	
	NSA (%)	IFSA(%)	NSA (%)	IFSA(%)
Faut1	96.33	97.67	95.33	45.33
Faut2	96.33	98.33	94.67	55.32
Faut3	96.33	98.47	94.67	35.27
Faut4	96.67	97.33	95.33	40.55
Faut5	96.33	95.67	94.67	50.78
Faut6	96.33	99.67	94.67	60.75
Faut7	96.33	95.45	95.33	55.42
Faut8	96.67	97.87	94.67	50.95
Faut9	96.33	96.85	95.33	61.55
Faut10	96.67	97.25	95.33	57.75
Faut11	96.67	99.43	95.33	58.25
Average Accuracy	96.45	97.64	95.03	51.99

NSA manifests the normal samples accuracy.
IFSA manifests the incipient fault samples accuracy.

TABLE 8. Fault detection accuracy with two types of test Stimuli.

Fault Sets	Multi-frequency test stimuli set & FFT		Pulse stimulus & Wavelet	
	NSA (%)	IFSA(%)	NSA (%)	IFSA(%)
Faut12	96.33	100.00	96.25	100.00
Faut13	96.33	100.00	95.67	100.00
Faut14	96.33	97.33	95.33	65.27
Faut15	96.67	98.33	96.33	77.25
Faut16	96.33	100.00	95.67	95.67
Average Accuracy	96.39	99.13	95.85	87.64

NSA manifests the normal samples accuracy.
IFSA manifests the incipient fault samples accuracy.

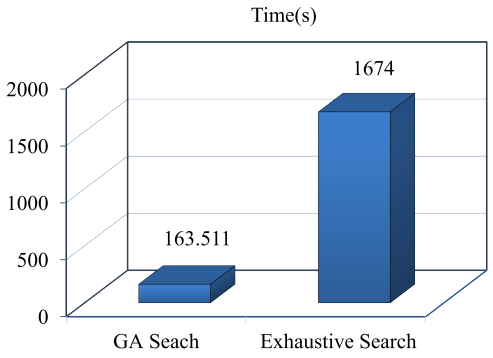

FIGURE 10. Comparison of the running time between the GA search and the exhaustive search.

B. SALLEN-KEY FILTER

The method of multi-frequency test generation is compared with another novel method mentioned in the literature [12], and its experimental circuit is the Sallen-key filter circuit shown in Fig. 1.

Sun *et al.* [12], the Sallen-key filter circuit consists of 4 resistors, 2 capacitors and 1 operational amplifier. The nominal values for all components are labeled in Fig. 1.

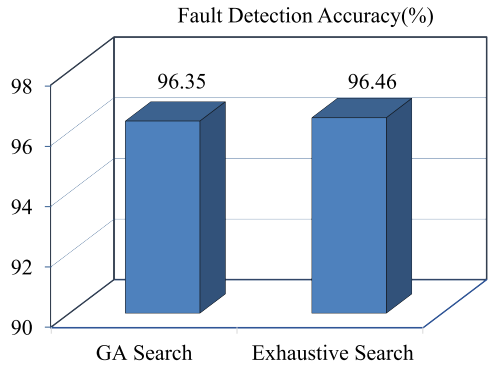

FIGURE 11. Comparison of the fault detection accuracy between the GA search and the exhaustive search.

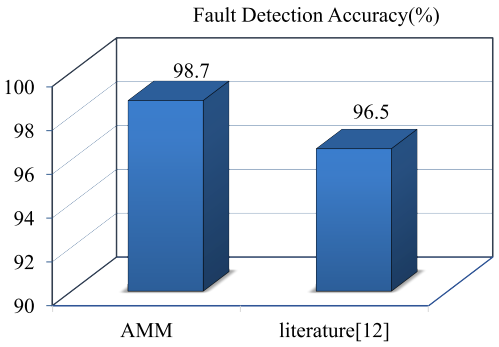

FIGURE 12. Comparison of average fault detection accuracy by different methods.

The tolerance of the resistors and capacitors are both set to 5%. The parametric deviations of all components causing faults are set to ±50%, and the type of fault is set as single, which forms 10 fault sets. The test stimuli will be selected using two different methods. Fault detection accuracy evaluates the validity of the methods based on the SVM fault classifier. The selected test stimuli set of the method mentioned in Sun *et al.* [12] are {5 KHz, 200 KHz, 80 KHz, 10 KHz, and 25 KHz}. However, using the method in this paper selects the test stimulus that is a single frequency of 6,856 Hz. Fig. 12 describes the comparison results of the average fault detection accuracy using different methods, and they indicate that the test stimulus obtained by the method in this paper has the lower number of test frequencies and the higher average fault detection accuracy than the homogeneous method in [12], which demonstrates that the method proposed in this paper has a better effectiveness and practicability.

IV. HARDWARE EXPERIMENT

The experimental environment of the software is too ideal to simulate the real environment where a circuit operates. This paper builds a hardware experiment platform to verify the effectiveness of the multi-frequency test stimuli using the incipient fault detection accuracy. Fig. 13 and Fig. 14 show the Leapfrog filter hardware circuit and the experiment platform.

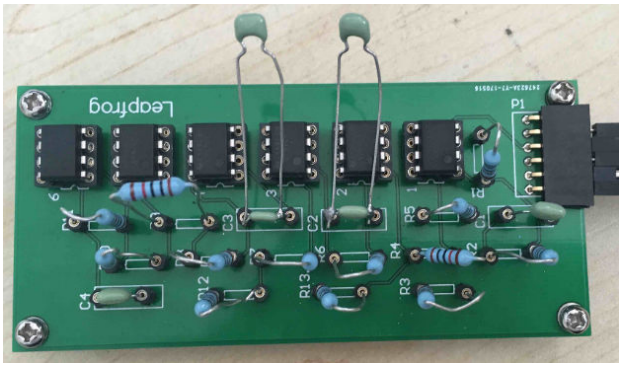

FIGURE 13. Leapfrog filter hardware circuit.

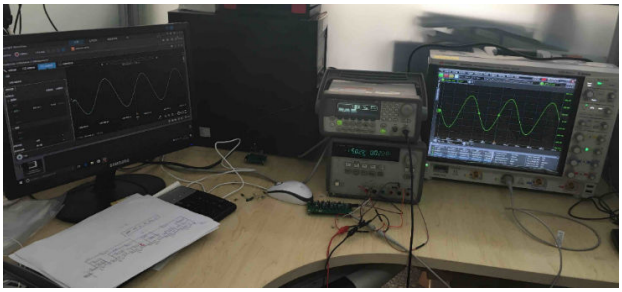

FIGURE 14. Hardware experiment platform.

TABLE 9. Fault sets in hardware experiment.

Fault	Number of fault components	Fault type	Fault components	Parameter deviation ratio
Faut1	Single	Incipient	C1	-10%
Faut2	Single	Incipient	C3	-9%
Faut3	Single	Incipient	R6	+10%
Faut4	Single	Incipient	R11	+12%
Fault5	Multiple	Incipient	C2	-12%
			R5	+15%
Fault6	Multiple	Incipient	R3	+11%
			R8	+15%
Fault7	Multiple	Incipient	R4	+14%
			R10	+13%
Fault8	Multiple	Incipient	R7	+15%
			R13	+10%
Faut9	Single	Serious	C2	-80%
Faut10	Single	Serious	C4	-55%
Faut11	Single	Common	C1	+32%
Faut12	Single	Common	R4	+25%
Faut13	Single	Common	R12	+45%

The hardware experiment platform consists of several major instruments. The DC signal source Agilent E3631A supplies the ±15 V power to the amplifiers, the signal generator Agilent 33220A generates the input signals corresponding to the multi-frequency test stimuli set, and the oscilloscope Keysight MOS404A is used to export the output data into the computer. Table 9 indicates the fault sets injected into the hardware circuit.

First, the signal generator provides sine waves based on the multi-frequency test stimuli set. Then, the output time domain signals are exported and stored in the computer using

TABLE 10. Incipient fault detection accuracy in hardware experiment.

Fault Sets	Multi-frequency test stimuli set & FFT		Pulse stimulus & Wavelet	
	NSA (%)	IFSA(%)	NSA (%)	IFSA(%)
Faut1	95.67	95.25	94.33	40.35
Faut2	95.67	95.43	93.67	50.34
Faut3	95.67	95.32	93.25	45.25
Faut4	95.89	94.65	92.33	43.15
Faut5	95.33	96.12	93.17	48.75
Faut6	94.65	94.75	92.67	55.65
Faut7	96.67	96.25	93.43	47.42
Faut8	95.65	95.35	94.35	45.95
Average Accuracy	95.63	95.39	93.40	47.11

NSA manifests the normal samples accuracy.
IFSA manifests the incipient fault samples accuracy.

TABLE 11. Fault detection accuracy in hardware experiment.

Fault Sets	Multi-frequency test stimuli set & FFT		Pulse stimulus & Wavelet	
	NSA (%)	IFSA(%)	NSA (%)	IFSA(%)
Faut9	96.33	100.00	95.33	100.00
Faut10	96.67	100.00	95.57	100.00
Faut11	96.67	97.42	95.25	74.25
Faut12	96.89	96.65	95.33	63.27
Faut13	96.33	100.00	95.57	94.75
Average Accuracy	96.58	98.81	95.41	86.45

NSA manifests the normal samples accuracy.
IFSA manifests the incipient fault samples accuracy.

the oscilloscope. The number of output normal samples and fault samples for every fault are 200 and 100, respectively. After the feature extraction using the FFT, 100 extracted normal samples are used as the training set of the SVDD and 100 extracted faults samples and another 100 normal samples are used as the testing set. The comparison experiment is still set to a pulse stimulus combined with a wavelet analysis. The detection accuracy is shown in Table 10 and Table 11.

The results show that the average incipient fault detection accuracy reaches 95.39%, whereas that with the pulse stimulus reaches 47.11%. Thus, using the multi-frequency test stimuli set can increase the incipient fault detection accuracy by more than 48.28%. Meanwhile, the test stimuli set increases the hard and soft fault average detection accuracy to 98.81%. These results adequately demonstrate that the multi-frequency test stimuli can increase the detection accuracy for all types of faults, especially for incipient faults in an actual circuit; thus, this method has great practical value.

V. CONCLUSIONS

This paper presents a novel method of multi-frequency test generation for incipient faults based on the AMM. The model uses the AMA combined with the GA to select the test frequencies for every incipient fault. The multi-frequency test stimuli set without redundant frequencies for the entire circuit is generated by the GRA. The selected multi-frequency test stimuli set has the better excitation of the incipient fault than the general pulse stimulus, and it greatly increases the incipient fault detection accuracy. Meanwhile, the test stimuli set can excite the serious and common faults. Compared with the homogeneous method mentioned in Sun *et al.* [12], the selected test stimuli set has fewer elements and higher fault detection accuracy. When the multi-frequency test stimuli set is used in the hardware circuit, the average fault detection reaches 95.39%. All of the results demonstrate that this novel method can quickly obtain simplified multi-frequency test stimuli, and it remarkably excites the subtle features of the incipient fault and is beneficial for fault detection and diagnosis in analog circuits. The proposed method is appropriate for applications that require the rapid detection of incipient faults and has great practical value.

REFERENCES

[1] M. Hu, W. Hong, H. Geng, and Y. Shiyuan, "Soft fault diagnosis for analog circuits based on slope fault feature and BP neural networks," *Tsinghua Sci. Technol.*, vol. 12, no. 1, pp. 26–31, 2007.
[2] C. Wegener and M. P. Kennedy, "Hard-fault detection and diagnosis during the application of model-based data converter testing," *J. Electron. Testing*, vol. 23, no. 6, pp. 513–525, 2007.
[3] B. Han, J. Li, and H. Wu, "Diagnosis method for analog circuit hard fault and soft fault," *Telkomnika Indonesian, J. Elect. Eng.*, vol. 11, no. 9, pp. 5420–5426, 2013.
[4] C. S. Kulkarni, J. R. Celaya, K. Goebel, and G. Biswas, "Physics based degradation modeling and prognostics of electrolytic capacitors under electrical overstress conditions," AIAA Infotech., Grapevine, TX, USA, Tech. Rep. AIAA 2013-5137, 2013.
[5] C. Kulkarni, G. Biswas, X. Koutsoukos, K. Goebel, and J. Celaya, "Physics of failure models for capacitor degradation in DC–DC converters," in *Proc. Maintenance Rel. Conf.*, 2010, pp. 1–13.
[6] C. Kulkarni, G. Biswas, X. Koutsoukos, J. Celaya, and K. Goebel, "Integrated diagnostic/prognostic experimental setup for capacitor degradation and health monitoring," in *Proc. IEEE Autotestcon*, Sep. 2010, pp. 1–7.
[7] L. Milor and V. Visvanathan, "Detection of catastrophic faults in analog integrated circuits," *IEEE Trans. Comput.-Aided Design Integr. Circuits Syst.*, vol. 8, no. 2, pp. 114–130, Feb. 1989.
[8] G. Devarayanadurg and M. Soma, "Analytical fault modeling and static test generation for analog ICs," in *Proc. IEEE/ACM Int. Conf. Comput.-Aided Des.*, San Jose, CA, USA, Nov. 1994, pp. 44–47.
[9] H. Luo, W. Lu, Y. Wang, L. Wang, and X. Zhao, "A novel approach for analog fault diagnosis based on stochastic signal analysis and improved GHMM," *Measurement*, vol. 81, pp. 26–35, Mar. 2016.
[10] B. Long, W. Xian, M. Li, and H. Wang, "Improved diagnostics for the incipient faults in analog circuits using LSSVM based on PSO algorithm with Mahalanobis distance," *Neurocomputing*, vol. 133, pp. 37–48, Jun. 2014.
[11] C. V. Marin, "Selecting optimum test frequency in dictionary of fault techniques," *Revue Roumaine Sci. Techn.*, vol. 56, no. 1, pp. 79–88, 2011s.
[12] Y. Sun, L. Ma, N. Qin, M. Zhang, and Q. Lv, "Analog filter circuits feature selection using MRMR and SVM," in *Proc. IEEE Int. Conf. Control, Autom. Syst.*, Oct. 2014, pp. 1543–1547.
[13] M. Bentobache, A. Bounceur, R. Euler, Y. Kieffer, and S. Mir, "New techniques for selecting test frequencies for linear analog circuits," in *Proc. IFIP/IEEE Int. Conf. Very Large Scale Integr.*, Oct. 2013, pp. 90–95.
[14] Z. Kincl and Z. Kolka, "Test frequency selection for overdetermined system of fault equations," in *Proc. 23rd Int. Conf. Radioelektronika (RADIOELEKTRONIKA)*, Apr. 2013, pp. 115–118.
[15] C. Yang, J. Yang, Z. Liu, and S. Tian, "Complex field fault modeling-based optimal frequency selection in linear analog circuit fault diagnosis," *IEEE Trans. Instrum. Meas.*, vol. 63, no. 4, pp. 813–825, Apr. 2014.
[16] G. Puvaneswari and S. Umamaheswari, "Test point selection and multiple soft faults detection in linear analog circuits based multiple frequency measurements," *Indian J. Res.*, vol. 7, no. 4, pp. 42–46, 2015.

[17] B. Muldrey, S. Deyati, and A. Chatterjee, "Concurrent stimulus and defect magnitude optimization for detection of weakest shorts and opens in analog circuits," in *Proc. IEEE Asian Test Symp.*, Nov. 2016, pp. 96–101.
[18] D. S. Liu and C. Y. Ni, "A study on the electrical resistance of solder joint interconnections," *Microelectron. Eng.*, vol. 63, no. 4, pp. 363–372, 2002.
[19] J. Gu, C. T. Lim, and A. A. O. Tay, "Equivalent solder joint and equivalent layer models for the simulation of solder column failure under drop impact," in *Proc. IEEE Electron. Packaging Technol. Conf. (EPTC)*, Dec. 2004, pp. 547–552.
[20] J. K. Park, Y. K. Byun, and J. T. Kim, "Equivalent electric circuit modeling of differential structures in PCB with genetic algorithm," in *Knowledge-Based Intelligent Information and Engineering Systems* (Lecture Notes in Computer Science), vol. 4253. Berlin, Germany: Springer-Verlag, 2006, pp. 907–913.

YANG YU (M'11) received the B.S., M.S., and Ph.D. degrees from the Department of Automatic Test and Control, Harbin Institute of Technology (HIT), Harbin, China, in 2002, 2004, and 2008, respectively.

From 2015 to 2016, she was a Visiting Scholar with Duke University, Durham, NC, USA. She is currently an Associate Professor with the Department of Automatic Test and Control, School of Electrical Engineering and Automation, HIT. She has authored over 30 publications in major journals and conference proceedings on electronic test technology and holds 21 granted China patents. Her current research interests include automatic testing, test technology for 3-D ICs, and diagnostic and prognostics for electronic systems.

YUEMING JIANG received the B.S. and M.S. degrees in measuring and control technology and instrumentation from the Harbin University of Science and Technology, Harbin, China, in 2011 and 2014, respectively. She is currently pursuing the Ph.D. degree in electrical engineering and automation with the Harbin Institute of Technology, Harbin.

Her research interests include the detection and diagnosis of incipient fault in analog circuit, feature selection of analog fault, and component degradation modeling.

XIYUAN PENG received the Ph.D. degree in instrumentation science and technology from the Harbin Institute of Technology (HIT), Harbin, China, in 1992.

He is currently a Full Professor with the Department of Automatic Test and Control, School of Electrical Engineering and Automation, HIT, where he is also the Dean. His current research interests include automatic test technologies, advanced diagnostics, and prognostics.